Tensile strength retention of glass fibre-reinforced stirrups subjected to aggressive solutions

Effect of environmental condition, stirrup shape and stirrup diameter

Hajmoosa, Amirhossein; Mahmoudi, Mussa; Ebrahimzadeh, Mohsen; Shakiba, Milad; Bazli, Milad

Published in:
Materials and Structures/Materiaux et Constructions

DOI:
10.1617/s11527-024-02306-0

Published: 01/03/2024

Document Version
Publisher's PDF, also known as Version of record

Citation for published version (APA):
Hajmoosa, A., Mahmoudi, M., Ebrahimzadeh, M., Shakiba, M., & Bazli, M. (2024). Tensile strength retention of glass fibre-reinforced stirrups subjected to aggressive solutions: Effect of environmental condition, stirrup shape and stirrup diameter. *Materials and Structures/Materiaux et Constructions*, *57*(2), 1-18. Article 31. https://doi.org/10.1617/s11527-024-02306-0

Mater Struct (2024) 57:31
https://doi.org/10.1617/s11527-024-02306-0

ORIGINAL ARTICLE

Tensile strength retention of glass fibre-reinforced stirrups subjected to aggressive solutions: effect of environmental condition, stirrup shape and stirrup diameter

Amirhossein Hajmoosa · Mussa Mahmoudi · Mohsen Ebrahimzadeh · Milad Shakiba · Milad Bazli

Received: 10 July 2023 / Accepted: 18 January 2024

Abstract The aim of this study was to examine how the tensile strength of glass fibre reinforced polymer stirrups is affected by different types of solutions, including alkaline, seawater, tap water, and acidic solutions. The study involved the production and testing of 260 stirrups in two different shapes (L and U) with diameters of 6 and 8 mm. The stirrups were immersed in different solutions for a period of 9 months at different temperatures (25, 40, and 60 °C). The findings indicated that the alkaline solution was the most aggressive environment, resulting in a maximum reduction of 92% in tensile strength after 9 months at 60 °C. Seawater and acidic solutions were the second and third most aggressive environments, causing maximum tensile strength reductions of 34 and 22% respectively, after 9 months at 60 °C. On the other hand, tap water was found to be the least aggressive environment, causing a maximum tensile strength reduction of 20% after 9 months at 60 °C. Furthermore, the study observed that the L-shaped stirrups exhibited slightly superior performance compared to the U-shaped stirrups. However, the diameter of the stirrups was found to be a negligible factor.

Keywords GFRP stirrup · Durability · Alkaline · Acid · Seawater · Accelerated ageing

1 Introduction

Fibre reinforced polymer (FRP) composites have found extensive use in a variety of civil and construction applications, particularly when employed to strengthen or enhance concrete structures [1–4]. The high strength and stiffness-to-weight ratio [5–9] and the absence of corrosion, make FRP a compelling alternative to traditional carbon steel in settings such as offshore structures [10–12].

Currently, the use of FRP bars as reinforcements within concrete structures is limited to a few structural components rather than being applied throughout the entire structure [13]. This limitation is due to the restricted availability of pre-curved or shaped FRP reinforcements in the market and their reduced structural performance compared to traditional steel reinforcements. Modern construction typically employs pre-bent and pre-cut steel bars

A. Hajmoosa · M. Mahmoudi (✉) · M. Shakiba
Department of Civil Engineering, Shahid Rajaee Teacher Training University, Lavizan, Tehran, Iran
e-mail: m.mahmoudi@sru.ac.ir

M. Ebrahimzadeh
Department of Civil Engineering, Sharif University of Technology, Tehran, Iran

M. Bazli (✉)
Faculty of Science and Technology, Charles Darwin University, Darwin, Australia
e-mail: milad.bazli@cdu.edu.au; m.bazli@uq.edu.au

M. Bazli
School of Mechanical and Mining Engineering, The University of Queensland, Brisbane, Australia

that are easily shaped through cold bending, unlike FRP reinforcements that lack an elastoplastic nature and may experience fibre buckling on the compression side when cold-bent [14]. A minor proportion of commercially accessible FRP bars are bent, and they are all pre-bent during the manufacturing process. Generally, the bends are formed when the material is in a partially cured state.

Despite the fact that FRP composites provide excellent protection against corrosion, they have been found to be vulnerable to some aggressive environments, particularly an alkaline environment, such as concrete [15–18]. The vulnerability of composite structures to harsh environments can become evident quickly, often within a short time of exposure. In some cases, even just a few days of exposure could lead to severe damage to the structure's mechanical strength or even cause catastrophic failure. An aggressive environment can bring about irreversible changes in the properties of polymer matrix composites [19]. Several types of tests are commonly used in experiments to assess the durability of FRP composites. These tests include exposure to alkaline, saline, and acidic solutions, as well as UV radiation, environmental cycles, and extreme temperatures [11, 15, 19–30]. A number of studies have been conducted that specifically examine the behaviour of GFRP bars and GFRP-reinforced concrete structures under various environmental conditions, including seawater [31, 32], alkaline [33, 34], and acidic [35].

GFRP composites can undergo various types of deterioration when exposed to aggressive environments. The degradation mechanisms typically involve the degradation of the resin matrix [36], damage to the fibre [37], and weakening of the fibre/resin interface [38]. Resin matrix degradation can result in swelling, delamination, plasticisation, cracking, and hydrolysis, especially, due to moisture absorption and chemical diffusion [39–42]. Meanwhile, damage to the glass fibre occurs when metallic cations are released from the fibre surface or when hydroxyl ions break the Si–O–Si bond through etching [43]. The degradation of the fibre/resin interface in FRP composites is mainly caused by matrix osmotic cracking, delamination, and fibre-resin debonding [44]. The deterioration of the interface is the primary cause of the degradation in the mechanical properties of FRP composites when exposed to aggressive environments [45].

The durability performance of GFRP composites in construction is still a challenge since their use is relatively new. To evaluate the durability of GFRP composites in harsh environments, accelerated ageing laboratory methods are frequently employed. Such tests typically involve immersing test samples in different solutions to imitate various environments, such as alkaline to simulate a concrete environment, acid to simulate an acidic environment, seawater to simulate an oceanic environment, and so on. Sometimes, higher temperatures are applied to speed up the rate of deterioration [1, 10, 11, 15, 19, 24, 26, 28, 46–49].

There have been numerous research studies examining the short-term and long-term structural performance of longitudinal FRP reinforcing bars. These studies have investigated both bare bars and bars embedded in concrete under different loading and environmental conditions. However, there has been little focus on the durability of bent FRP reinforcing bars under aggressive environments. Only a few number of research studies have examined the structural performance of reinforced concrete structures that are fully reinforced with FRP reinforcements [50, 51]. However, these studies typically only consider the overall degradation level of the entire structure and do not investigate the degradation level of the individual bent FRP reinforcements.

So far, there have been no investigations conducted on durability of bare GFRP stirrups under harsh conditions such as seawater, alkaline substances, and acidic substances. Therefore, the aim of this research is to address a knowledge gap by examining how the short-term tensile strength of GFRP stirrups is affected by exposure to different environmental conditions, including seawater, tap water, alkaline, and acidic solutions. The research consisted of producing and preparing 260 GFRP stirrups, and examining their tensile strength after undergoing conditioning for a period of 9 months at varying temperatures of 25, 40, and 60 °C. The experiment variables included U-shaped and L-shaped stirrups with diameters of 6 mm and 8 mm.

2 Experimental procedure

2.1 GFRP stirrups

The experiment utilised U and L-shaped GFRP stirrups with nominal diameters of 6 and 8 mm, which were helically wrapped (Fig. 1). These stirrups were made from E-glass fibres and vinyl ester resin, with a ratio of 70% fibres to 30% resin by volume. The mechanical properties of the bar were determined based on the nominal cross-sectional area, and the resulting values are presented in Table 1. The tensile tests were carried out in accordance with the guidelines of ASTM D7205/D7205M-21. [52].

Table 1 GFRP stirrup mechanical characteristics

Bar diameter (mm)	Cross section area (mm^2)	Density (g/cm^2)	Tensile strength (MPa)	Modulus of elasticity (GPa)
6	28.27	2.2	1100 ± 50	52.5 ± 2.5
8	50.27	2.2	1050 ± 50	52.5 ± 2.5

2.2 Environmental conditioning

In order to investigate how well the stirrups retain their tensile strength when exposed to harsh environmental conditions, they were put through a 9-month laboratory accelerated ageing. During this time, the stirrups were exposed to 13 different conditions, including: (1) Laboratory ambient weather as the reference condition (L-25 °C), (2) Immersion in tap water at ambient temperature (T-25 °C), (3) Immersion in tap water at 40 °C (T-40 °C), (4) immersion in tap water at 60 °C (T-60 °C), (5) Immersion in seawater at ambient temperature (SW-25 °C), (6) Immersion in seawater at 40 °C (SW-40 °C), (7) Immersion in seawater at 60 °C (SW-60 °C), (8) Immersion in alkaline solution at ambient temperature (AL-25 °C), (9) Immersion in alkaline solution at 40 °C (AL-40 °C), (10) immersion in alkaline solution at 60 °C

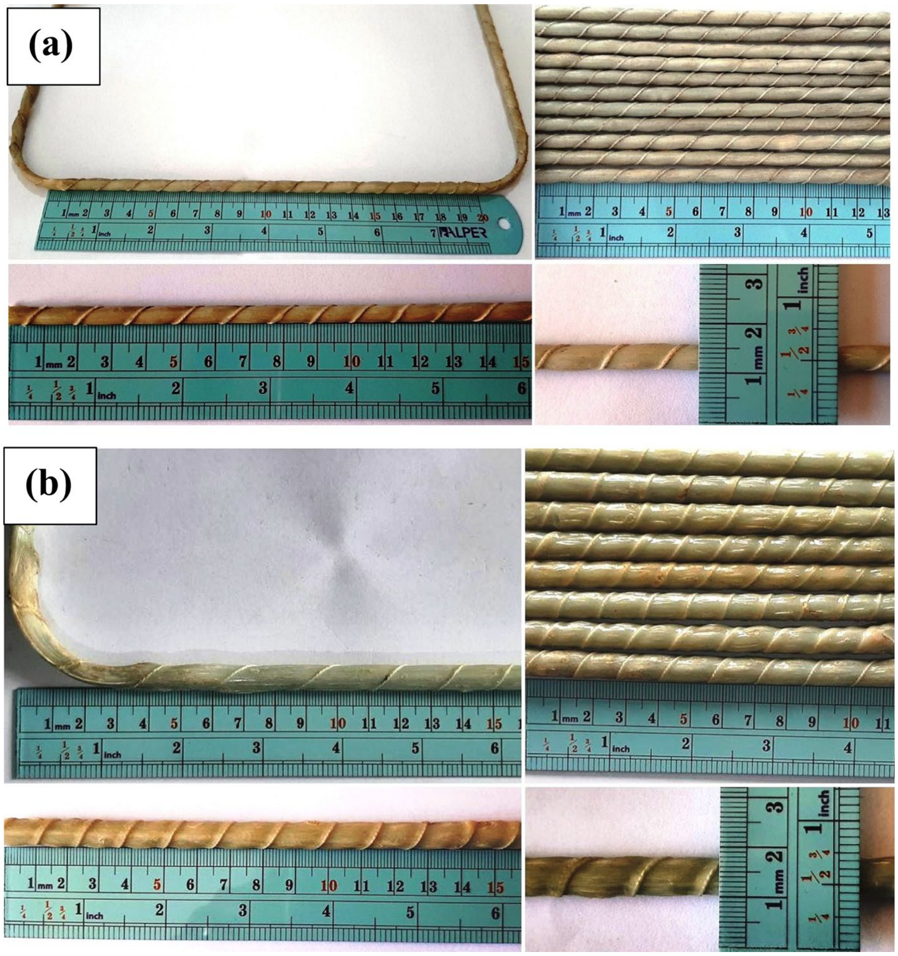

Fig. 1 GFRP stirrups: **a** 6 mm, and **b** 8 mm

(AL-60 °C), (11) Immersion in acidic solution at ambient temperature (AC-25 °C), (12) Immersion in acidic solution at 40 °C (AC-40 °C), (13) Immersion in acidic solution at 60 °C (AC-60 °C).

Numerous research papers have utilised an alkaline solution (a mixture of chemicals dissolved in distilled water) to replicate the actual concrete environment, with the same chemical compositions as the concrete being studied [19, 53–55]. Researchers have also employed acidic solutions to replicate the corrosive environment of polluted industrial areas and corrosive fluids [19, 56].

Similarly to prior research [32, 57], accelerated ageing temperatures of up to 60 °C were employed for conditioning in this study. This temperature was intentionally kept below the glass transition temperature of the resin to avoid inducing degradation rather than just accelerating it [58].

Alkaline solution was prepared by dissolving 19.6 g/L of potassium hydroxide (KOH), 2.4 g of sodium hydroxide (NaOH), and 2 g/L of calcium hydroxide ($Ca(OH)_2$) in distilled water. A solution with an acidic pH was created by dissolving 11.5 mg/L hydrochloric acid (HCl) in distilled water. The seawater was designed to mimic the chemical composition of water found in the Persian Gulf. On average, the alkaline, acidic, and seawater solutions had a pH of 13.5, 8.1, and 3.5, respectively. The pH of the solution was checked every week, and if it changed by more than 0.2, the entire solution was replaced. The specific chemical compositions of the simulated seawater used in this study are outlined in Table 2. Table 3 provides a detailed overview of the test plan and the identification system used for the samples.

2.3 Test set-up

To determine the bent tensile strength of U and L-shaped GFRP stirrups, two fixtures were manufactured and installed onto a Zwick Roell universal testing machine with a maximum load capacity of 150 kN. The testing was performed using a displacement-controlled loading method at a speed of 1 mm/min. U-shaped stirrups were tested according to set-up proposed by ACI 440.3R-12 [59] (B.12: Test method for determining effect of corner radius on tensile strength of FRP bars). The testing setup comprises two sections: an upper portion and a lower portion that encircle the FRP bar. The upper section serves as the testing area and is equipped with replaceable corner inserts positioned at its two corners. The lower section is responsible for anchoring the specimen by means of anchors. The assembly is held together during specimen installation through the use of two bolts and two steel rods securing the upper and lower fixture sections. The tensile loading fixture is affixed to the upper cross-head of the testing machine, and the upper test fixture is linked to the tensile loading fixture by means of a steel rod inserted through holes in the upper section. The lower section of the test fixture is positioned on the lower plate of the testing machine using a threaded steel bar and two nuts. The test setup used for testing L-shaped stirrups is a modified version of the one originally used for U-shaped stirrups.

The set-up used for the test is illustrated in Fig. 2.

Table 2 Chemical compositions of simulated seawater

NaCl (gr/lit)	$MgCl_2$ (gr/lit)	$CaCl_2$ (gr/lit)	KCl (gr/lit)	KBr (gr/lit)
27.50	5.10	1.11	0.76	0.10

3 Results and discussion

3.1 Failure mode

As expected, both the controlled and conditioned samples failed due to the bending stress in the bent area. In the vicinity of the bend zone, a localised stress concentration is observed due to the curvature of the stirrup. This stress concentration is further intensified by the inherent weakness of the fibres in the transverse direction and the alteration in fibre orientation, particularly in the innermost layer of fibres [60]. The decreased strength of the curved segment, combined with the heightened stress concentration during loading, initiates the formation of cracks within the deformed region (Fig. 3a). Subsequently, these cracks propagate toward the straight portion of the stirrup (Fig. 3b). During this phase, although separate fibres still bear some of the applied loads, albeit with a considerable reduction in stiffness, the sharp edges of the crack (at the microscopic level) might induce failure of the fibres. Ultimately, the fracture of these fibres results in the failure of the stirrup

Table 3 Test plan and sample identification system

Conditioning type	Stirrup diameter	Stirrup shape	Exposure temperature (°C)	Sample convention	Number of identical tests
Laboratory condition	6	U shape	25	L-U-6-25	5
	8	U shape	25	L-U-8-25	5
	6	L shape	25	L-L-6-25	5
	8	L shape	25	L-L-8-25	5
Tap water	6	U shape	25	T-U-6-25	5
	8	U shape	25	T-U-8-25	5
	6	L shape	25	T-L-6-25	5
	8	L shape	25	T-L-8-25	5
	6	U shape	40	T-U-6-40	5
	8	U shape	40	T-U-8-40	5
	6	L shape	40	T-L-6-40	5
	8	L shape	40	T-L-8-40	5
	6	U shape	60	T-U-6-60	5
	8	U shape	60	T-U-8-60	5
	6	L shape	60	T-L-6-60	5
	8	L shape	60	T-L-8-60	5
Seawater solution	6	U shape	25	SW-U-6-25	5
	8	U shape	25	SW-U-8-25	5
	6	L shape	25	SW-L-6-25	5
	8	L shape	25	SW-L-8-25	5
	6	U shape	40	SW-U-6-40	5
	8	U shape	40	SW-U-8-40	5
	6	L shape	40	SW-L-6-40	5
	8	L shape	40	SW-L-8-40	5
	6	U shape	60	SW-U-6-60	5
	8	U shape	60	SW-U-8-60	5
	6	L shape	60	SW-L-6-60	5
	8	L shape	60	SW-L-8-60	5
Alkaline solution	6	U shape	25	AL-U-6-25	5
	8	U shape	25	AL-U-8-25	5
	6	L shape	25	AL-L-6-25	5
	8	L shape	25	AL-L-8-25	5
	6	U shape	40	AL-U-6-40	5
	8	U shape	40	AL-U-8-40	5
	6	L shape	40	AL-L-6-40	5
	8	L shape	40	AL-L-8-40	5
	6	U shape	60	AL-U-6-60	5
	8	U shape	60	AL-U-8-60	5
	6	L shape	60	AL-L-6-60	5
	8	L shape	60	AL-L-8-60	5

Table 3 (continued)

Conditioning type	Stirrup diameter	Stirrup shape	Exposure temperature (°C)	Sample convention	Number of identical tests
Acidic solution	6	U shape	25	AC-U-6-25	5
	8	U shape	25	AC-U-8-25	5
	6	L shape	25	AC-L-6-25	5
	8	L shape	25	AC-L-8-25	5
	6	U shape	40	AC-U-6-40	5
	8	U shape	40	AC-U-8-40	5
	6	L shape	40	AC-L-6-40	5
	8	L shape	40	AC-L-8-40	5
	6	U shape	60	AC-U-6-60	5
	8	U shape	60	AC-U-8-60	5
	6	L shape	60	AC-L-6–60	5
	8	L shape	60	AC-L-8-60	5
Total					260

(Fig. 3c). It is worth noting that the type of conditioning and the shape of the stirrup (U or L) did not affect the observed failure mode.

3.2 Tensile strength retention

The ultimate tensile stress developed in U-shaped and L-shaped GFRP stirrups is calculated using Eqs. (1) and (2), respectively.

$$f_u = \frac{F_{\max}}{2A} \tag{1}$$

$$f_u = \frac{\sqrt{2}F_{\max}}{2A} \tag{2}$$

where $F_{\max}$ is the maximum applied load by the machine and A is the nominal cross-section area (one leg) of the stirrup.

The results of the tensile tests are presented in Table 4. The subsequent sections will provide a detailed discussion on the impact of the conditioning environment, stirrup shape, and diameter on the tensile stress development, using the average values obtained from five identical tests for each sample for comparison and discussion.

3.3 Effect of environmental conditions

Figure 4 compares the GFRP stirrups' ultimate tensile stress retention with respect to the environmental conditions. The extent of damage resulting from exposure to harsh environments is influenced by various factors, including exposure conditions, time, temperature, as well as the type of fibre and resin used, along with their chemical composition.

According to Fig. 4, it was observed that the alkaline environment was considerably more aggressive than other environments, resulting in a reduction of up to 82, 86, and 92% in tensile strength, respectively after being exposed to temperatures of 25, 40, and 60 °C for a duration of 9 months, regardless of the shape and diameter of the stirrup used. This significant decrease in strength indicates that stirrups are much more susceptible to damage from alkaline conditions than longitudinal bars [36, 46]. The main factor causing this is that the load-carrying capacity of fibres in curved areas is greatly diminished, leading to a high dependence on the resin and composite delamination and therefore affecting the mechanical strength of GFRP stirrups. It is a commonly accepted fact that mechanical properties which are mainly controlled by the resin and resin-fibre delamination, such as interlaminar shear strength, are more prone to damage in

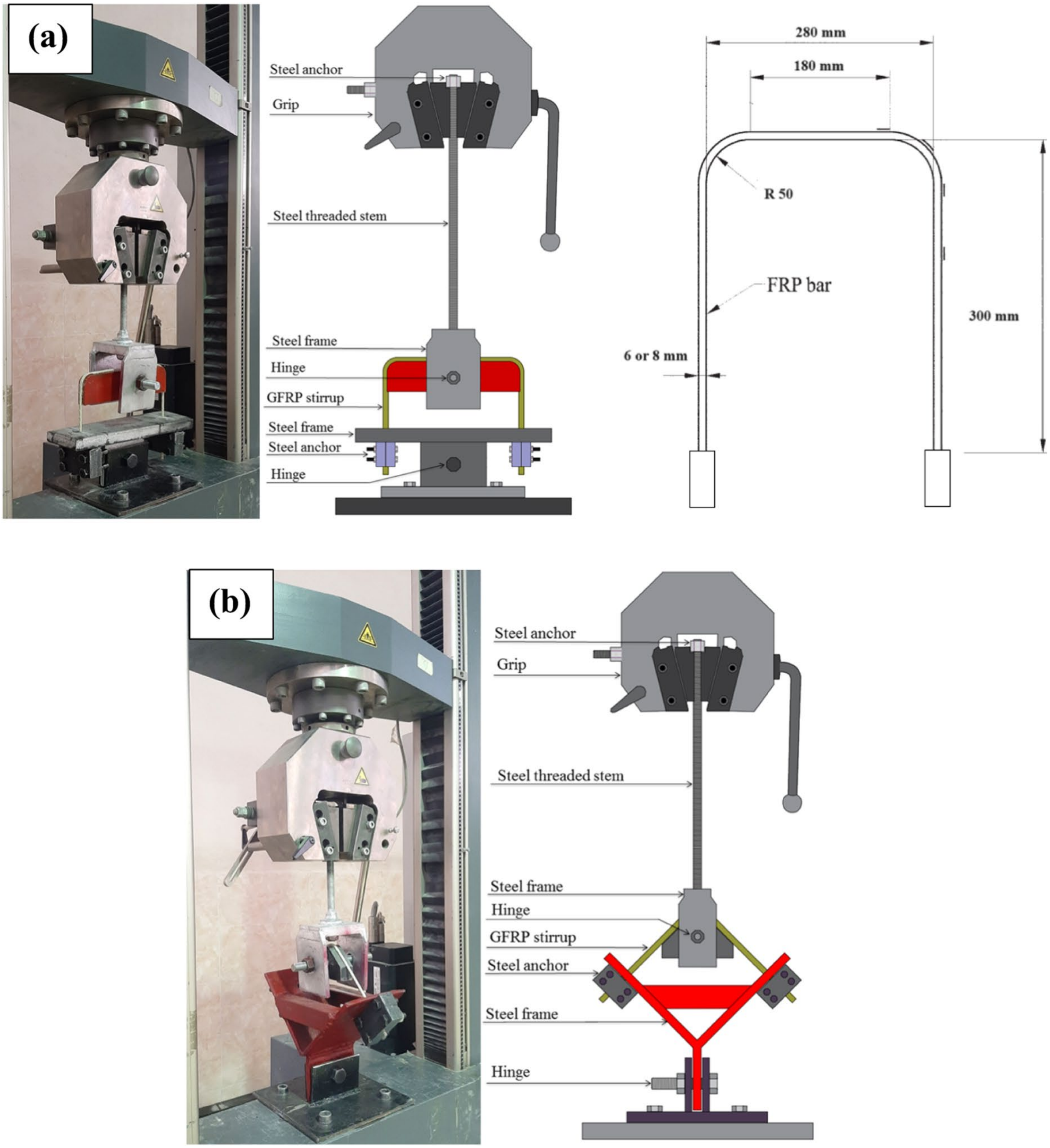

Fig. 2 Test set-up: **a** Testing configuration of U-shaped stirrup specimens, and **b** Testing configuration of L-shaped stirrup specimens

harsh conditions compared to mechanical properties which are less influenced by the resin, such as the tensile strength along the direction of the fibres [61].

When GFRP composites are subjected to alkaline environments, multiple mechanisms of degradation occur, resulting in fibre-resin debonding. The weakening and loss of mechanical properties in GFRP profiles due to exposure to solutions are caused by either physical or chemical reactions between. The diffusion of the solution into the GFRP material

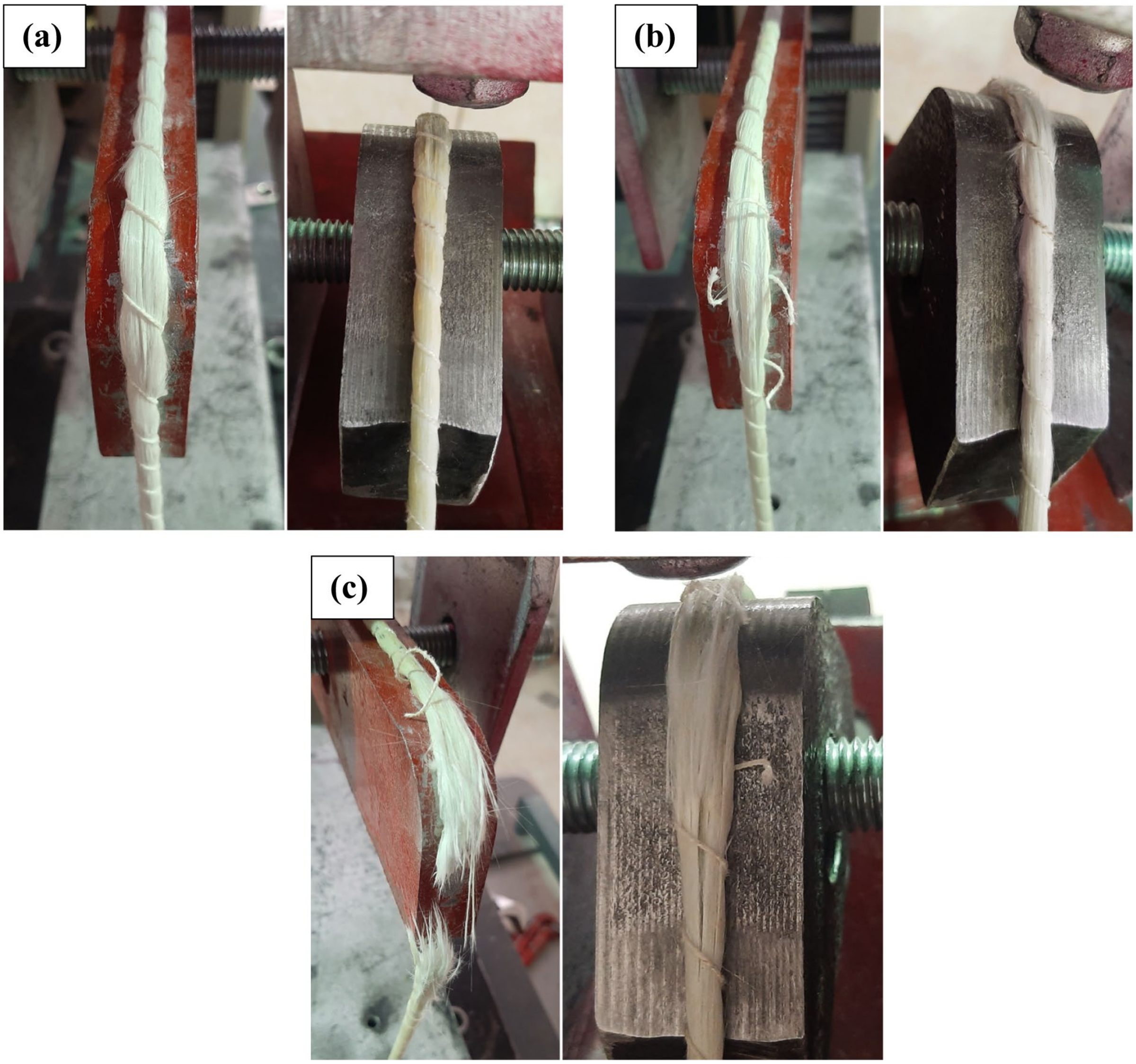

Fig. 3 Failure modes of U and L-shaped GFRP stirrups during tests

results in an increase in the volume of the resin matrix, which leads to the formation of microcracks at the interface between the fibres and matrix. These microcracks weaken the adhesion between the fibres and matrix, causing a degradation of the bond between the two components. This ultimately leads to a reduction in the overall mechanical properties of the GFRP composite [62, 63]. The severity of the damage caused is contingent upon factors such as the type of solution, the level of solution penetration, and the constitution of the fibres. In glass fibres, it is suggested that the main cause of corrosion shell formation on fibres in an alkali environment is the reaction between alkali-ions and silicate in glass fibres, which causes network destruction and gradual dissolution. This reaction can be seen in Eqs. (3) and (4), which also show the subsequent destruction and dissolution of the silicate network. As the corrosion shells thicken over time and move through the fibre core, insoluble compounds such as calcium, iron, titanium, magnesium and zirconium are left behind. The expansion of corrosion shells

Table 4 Test results summary

Sample convention	f_u(MPa)						COV (%)	Retention (%)
	SP1	SP2	SP3	SP4	SP5	Average		
L-U-6-25	303.4	311.1	307.7	313.7	302.8	307.7	1.4	100.0
L-U-8-25	354.9	361.2	357.0	359.6	350.2	356.6	1.1	100.0
L-L-6-25	294.6	291.1	290.1	299.7	290.9	293.3	1.2	100.0
L-L-8-25	343.1	354.9	343.9	351.4	351.9	349.0	1.3	100.0
T-U-6-25	281.7	275.7	277.9	269.8	282.5	277.5	1.7	90.2
T-U-8-25	309.4	314.2	322.3	317.3	312.3	315.1	1.4	88.4
T-L-6-25	275.3	278.4	281.4	281.6	279.4	279.2	0.8	95.2
T-L-8-25	328.2	346.1	333.7	337.5	339.6	337.0	1.8	96.6
T-U-6-40	271.7	269.4	261.5	258.0	267.1	265.6	1.9	86.3
T-U-8-40	308.5	295.7	310.3	302.1	297.4	302.8	1.9	84.9
T-L-6-40	272.6	253.6	264.8	268.2	271.0	266.0	2.5	90.7
T-L-8-40	319.7	325.6	337.2	322.8	339.5	328.9	2.4	94.3
T-U-6-60	252.3	247.8	255.6	240.7	243.0	247.9	2.2	80.6
T-U-8-60	280.9	287.8	276.0	285.2	290.5	284.1	1.8	79.7
T-L-6-60	226.2	236.6	260.3	240.5	262.5	245.2	5.7	83.6
T-L-8-60	317.6	304.1	309.2	300.5	312.3	308.7	1.9	88.5
SW-U-6-25	234.6	244.1	239.7	238.9	236.6	238.8	1.3	77.6
SW-U-8-25	266.9	257.2	250.8	259.3	265.9	260.0	2.3	72.9
SW-L-6-25	224.5	243.4	244.4	227.3	248.2	237.6	4.1	81.0
SW-L-8-25	292.5	302.0	298.2	294.0	303.6	298.1	1.5	85.4
SW-U-6-40	233.2	225.4	222.7	235.4	229.2	229.2	2.1	74.5
SW-U-8-40	253.0	244.1	236.2	240.6	247.9	244.4	2.4	68.5
SW-L-6-40	224.2	246.3	235.7	226.9	225.5	231.7	3.6	79.0
SW-L-8-40	284.9	300.1	294.2	296.4	288.6	292.8	1.9	83.9
SW-U-6-60	214.7	212.4	225.1	220.7	216.9	217.9	2.1	70.8
SW-U-8-60	234.7	243.4	225.6	230.9	242.4	235.4	2.9	66.0
SW-L-6-60	206.5	227.1	225.6	214.9	211.1	217.0	3.7	74.1
SW-L-8-60	270.0	289.4	277.7	273.3	291.4	280.4	3.1	80.3
AL-U-6-25	65.2	63.7	64.8	61.2	63.0	63.6	2.2	20.7
AL-U-8-25	64.4	62.3	64.1	60.8	63.0	62.9	2.1	17.7
AL-L-6-25	69.9	73.1	63.8	74.5	76.5	71.6	6.2	24.4
AL-L-8-25	93.3	95.5	98.5	98.1	100.1	97.1	2.5	27.8
AL-U-6-40	49.7	52.7	50.7	49.1	51.7	50.8	2.5	16.5
AL-U-8-40	51.8	49.3	49.9	49.6	52.7	50.7	2.6	14.2
AL-L-6-40	52.4	56.5	55.0	55.9	52.9	54.6	3.0	18.6
AL-L-8-40	73.7	80.7	75.6	80.4	72.7	76.6	4.3	22.0
AL-U-6-60	28.8	31.5	31.2	29.5	29.0	30.0	3.8	9.8
AL-U-8-60	32.1	34.8	33.0	34.5	32.6	33.4	3.2	9.4
AL-L-6-60	21.3	27.6	22.7	23.9	26.3	24.3	9.5	8.3
AL-L-8-60	42.0	39.7	45.1	39.5	44.7	42.2	5.7	12.1
AC-U-6-25	272.5	265.3	267.3	279.2	276.6	272.2	1.9	88.4
AC-U-8-25	314.8	298.4	307.7	309.2	299.4	305.9	2.0	85.8
AC-L-6-25	267.4	273.9	267.9	279.5	282.4	274.2	2.2	93.5
AC-L-8-25	325.8	338.8	335.7	328.0	341.4	333.9	1.8	95.7
AC-U-6-40	267.7	258.7	252.2	255.6	263.5	259.5	2.1	84.3

Table 4 (continued)

Sample convention	f_u(MPa)						COV (%)	Retention (%)
	SP1	SP2	SP3	SP4	SP5	Average		
AC-U-8-40	285.4	292.3	301.7	287.1	298.0	292.9	2.1	82.1
AC-L-6-40	252.7	271.9	258.8	252.2	265.3	260.2	2.9	88.7
AC-L-8-40	328.5	319.7	315.0	325.0	322.3	322.1	1.4	92.3
AC-U-6-60	240.9	247.8	234.0	238.8	239.6	240.2	1.9	78.1
AC-U-8-60	275.4	284.8	267.3	283.5	272.8	276.7	2.4	77.6
AC-L-6-60	229.0	246.3	238.1	227.6	237.0	235.6	2.9	80.3
AC-L-8-60	311.0	301.2	293.5	306.5	298.5	302.1	2.0	86.6

creates local stress in the matrix, which can lead to fibre/resin interface debonding and exfoliation from fibres.

$$\equiv Si - OR + \left(H^{+} + OH^{-}\right) \rightarrow \equiv Si - OH + ROH \tag{3}$$

$$\equiv Si - O - Si \equiv + \left(R^{+} + OH^{-}\right) \rightarrow \equiv Si - OH + RO - Si \tag{4}$$

Seawater was found to be the second most damaging environment for GFRP stirrups after exposure to an alkaline environment. However, the extent of strength reduction in GFRP stirrups was significantly lower in seawater than in an alkaline environment. The maximum reductions in strength were 27, 31, and 34% after 9 months of immersion at temperatures of 25, 40, and 60 °C, respectively. When GFRP composites are immersed in seawater, apart from the damaging impact caused by the diffusion of the solution into the composite, they can develop blisters and solid compounds on their surfaces. Blisters can occur due to osmotic pressures that build up between the GFRP surface and the seawater, while the formation of solid compounds suggests a galvanic reaction between soluble compounds in the specimens and active metals in the solution. Blistering is a common occurrence in FRP materials when they are in contact with active metals in seawater. During immersion of GFRP composites in seawater solution, hydroxyl ions accumulate on the glass fibres and react with components in the solution such as sodium ions to balance the electrical charge, which creates an osmotic condition and increases the pressure from the sodium hydroxide. This phenomenon has the potential to cause the resin to deform, which may ultimately lead to a degradation in the mechanical properties of the composite [64].

Following seawater exposure, an acidic solution was found to be the next aggressive environment, with the maximum reductions in strength being 14, 18, and 22% after 9 months of immersion at temperatures of 25, 40, and 60 °C, respectively. Exposure to an acidic solution can result in a chemical attack that causes the ester groups of the matrix to undergo hydrolysis. Since these ester groups are located in the chain backbone of the polymer, this hydrolysis causes chain scission. The reduction in molecular weight due to this scission ultimately leads to a decrease in the mechanical properties of the composite. When the acid solution penetrates the composite through voids and cracks, there is an ionic exchange that occurs between metallic cations (such as Na + ions) at the surface of the glass and hydrogen ions. This results in the leaching of metallic cations from the outer layer of the fibres, followed by the release of Cl − ions, which diffuse quickly into the voids of the matrix and transfer into the interphase, thereby weakening the strength of the bonds. The release of Cl − ions and washing of fibre surfaces have a detrimental effect on the matrix and fibre/resin interfacial bond strength, gradually decreasing the mechanical properties of the GFRP composites [65].

As anticipated, tap water was the least aggressive environment compared to all other solutions, resulting in stirrups showing maximum strength reductions of only 12, 15, and 20% after being immersed for 9 months at temperatures of 25, 40, and 60 °C, respectively.

3.4 Effect of stirrup shape

Figure 5 compares the GFRP stirrups' ultimate tensile stress retention with respect to the stirrup shape. According to Fig. 5, all L-shaped stirrups

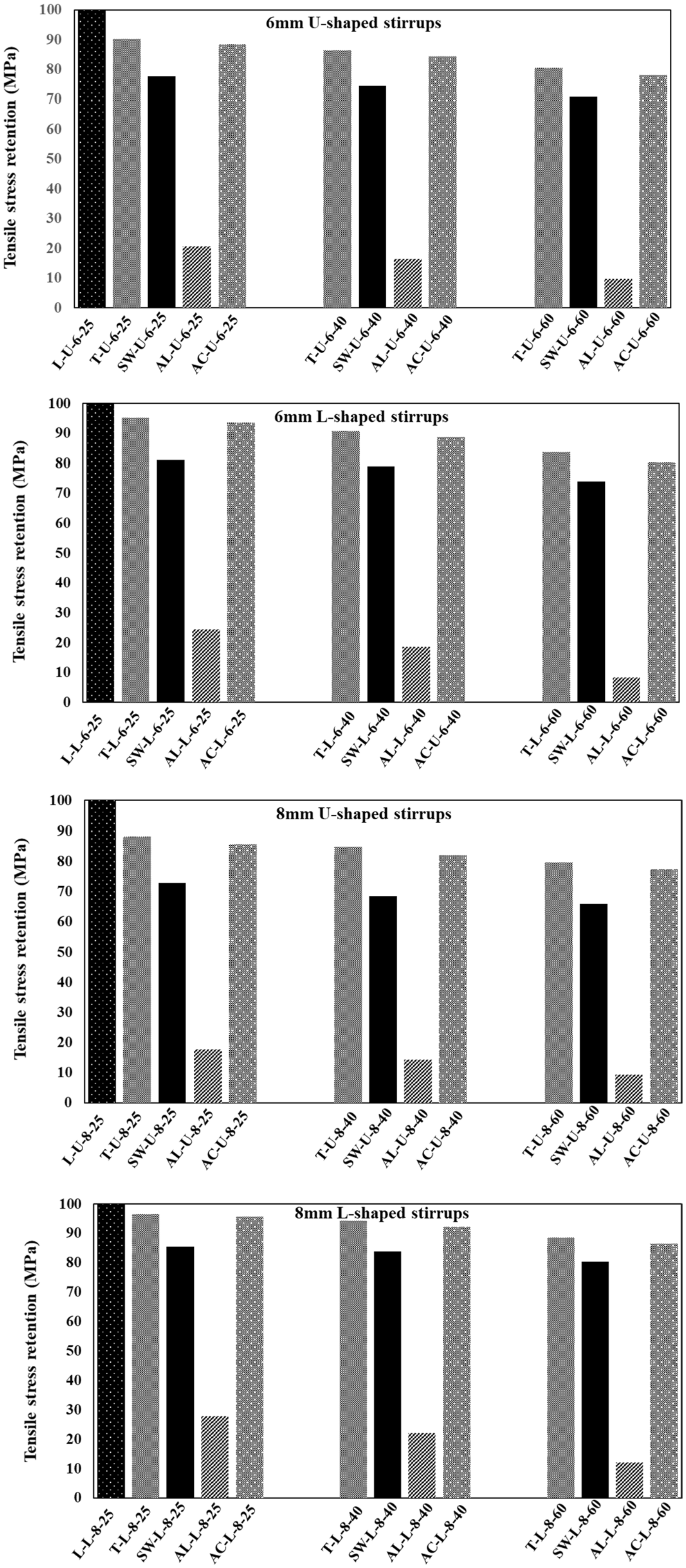

Fig. 4 Ultimate tensile stress retention with respect to the environmental condition

had higher strength retention values than U-shaped stirrups, regardless of their diameter or the environment they were exposed to, except for 6 mm stirrups in an alkaline environment at 60 °C. It's possible that U-shaped stirrups fail because they have two bent locations, and the one that fails first determines the overall failure. If the composite material degrades unevenly on both curved sides, this can cause an unbalanced load, leading to an earlier failure compared to an unconditioned U-shaped stirrup. The manufacturing quality and the test set-up configurations could be the other possible reasons for such differences between the U-shaped and L-shaped stirrups' strength retentions.

3.5 Effect of stirrup diameter

Figure 6 compares the GFRP stirrups' ultimate tensile stress retention with respect to the stirrup diameter. As illustrated in Fig. 6, the U-shaped stirrups exhibited slightly superior performance with 6 mm diameter compared to those with 8 mm diameter, whereas the opposite was observed in the case of L-shaped stirrups. The uniformity of the trend across all environmental conditions suggests that the manufacturing process may be the reason for the observed performance difference. However, because the discrepancies between the 6 and 8 mm stirrups are negligible in all cases, it can be inferred that the impact of stirrup diameter on their resilience in harsh environments is insignificant.

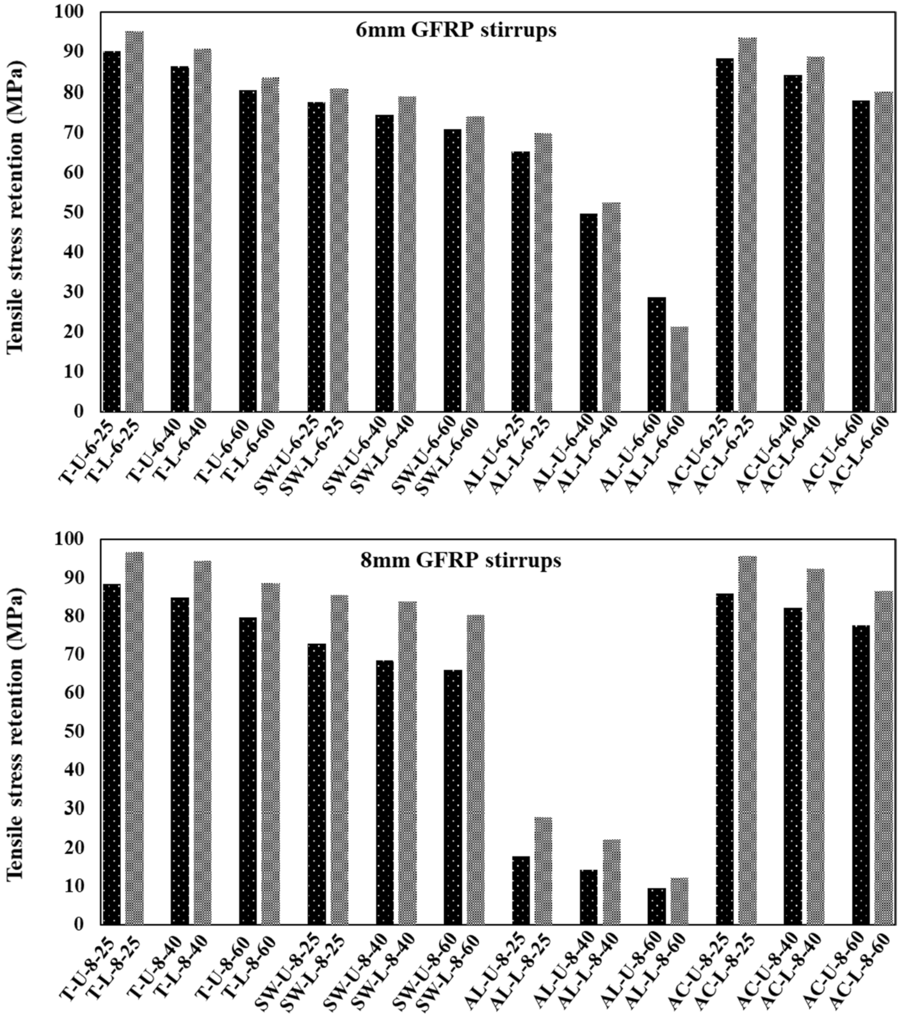

Fig. 5 Ultimate tensile stress retention with respect to the stirrup shape

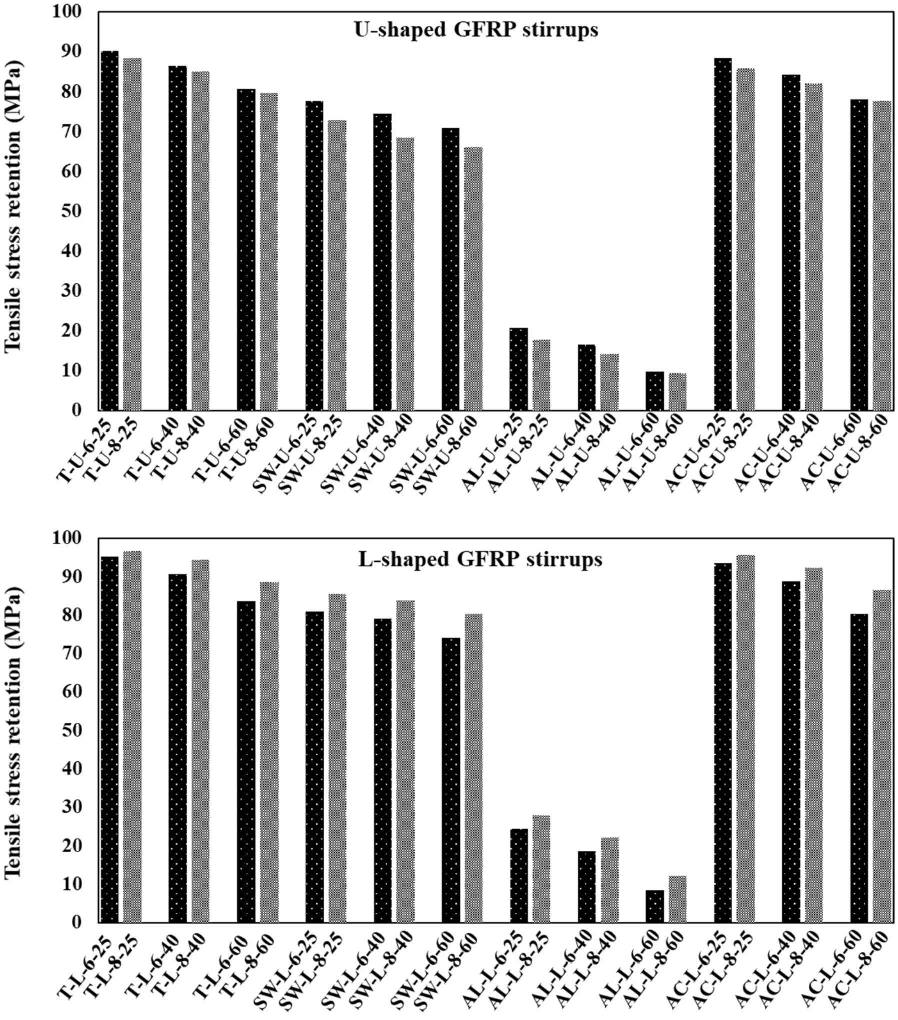

Fig. 6 Ultimate tensile stress retention with respect to the stirrup diameter

4 Parametric analysis: analysis of variance

To assess how different factors contribute to the tensile strength retention of GFRP stirrups when subjected to different environmental conditions, a two-way ANOVA was conducted. To avoid having excessive data, ANOVA analysis was conducted only on the 8 mm L-shaped stirrup size, since there was no significant difference observed between the results of the 6 and 8 mm and L-shaped and U-shaped stirrups.

Tables 5, 6 and 7 provide a summary of the ANOVA results for L-shaped 8 mm stirrups, taking into account the effects of the environmental condition and the conditioning temperature. It should be noted that in order to assess the degree of aggressiveness of each solution, the AL, AC, and SW solutions were analysed separately, along with tap water.

ANOVA Tables show the sum of squares (*SS*), degrees of freedom (*df*), mean square (*MS*), *F*, *P-value*, and critical *F*crit for each parameter. The *P-value* represents the probability of obtaining the *F* assuming the null hypothesis, and the *F*crit indicates the significance of the variable on the output.

As is seen in Tables 5 and 6, the *P-value* for both solution type and conditioning temperature are less than 0.05 (i.e. $F\ crit < F$). Therefore, it can be inferred that altering the environment from tap water to seawater or alkaline environments, as well as increasing the conditioning temperature, has an impact on the tensile strength retention of GFRP stirrups. However, the *P-value* for the conditioning solution in Table 7 is very close to 0.05 showing that changing the conditioning solution from tap water to acidic solution does not significantly affect the tensile strength retention

Table 5 Two-way ANOVA results for L-shaped 8 mm stirrups under tap water and seawater

Source of variation	*SS*	*df*	*MS*	*F*	*P-value*	*F crit*	Contribution (%)
Temperature	2800.8	2	1400.4	26.2	9.29E−07	3.4	21.3
Solution	8924.0	1	8924.0	166.8	2.68E−12	4.3	67.8
Interaction	150.6	2	75.3	1.4	0.26	3.4	1.2
Error	1283.7	24	53.5				9.7
Total	13,159.3	29					100.0

Table 6 Two-way ANOVA results for L-shaped 8 mm stirrups under tap water and alkaline solution

Source of variation	*SS*	*df*	*MS*	*F*	*P-value*	*F crit*	Contribution (%)
Temperature	8936.4	2	4468.2	136.4	7.83E−14	3.4	1.8
Solution	479,854.2	1	479,854.2	14,646.0	5.93E−35	4.3	97.8
Interaction	885.5	2	442.7	13.5	0.000117	3.4	0.2
Error	786.3	24	32.8				0.2
Total	490,462.5	29					100.0

Table 7 Two-way ANOVA results for L-shaped 8 mm stirrups under tap water and acidic solution

Source of variation	*SS*	*df*	*MS*	*F*	*P-value*	*F crit*	Contribution (%)
Temperature	4685.8	2	2342.9	48.8	3.45E−09	3.4	77.0
Solution	228.1	1	228.1	4.7	0.039229	4.3	3.7
Interaction	21.8	2	10.9	0.2	0.798180	3.4	0.4
Error	1150.9	24	47.9				18.9
Total	6086.6	29					100

of GFRP stirrups. In contrast to the solution effect, conditioning temperature was found to be an effective factor similar to other conditions (i.e. *P-value* < 0.05).

When comparing the impact of solution parameters among the three different aggressive solutions, it was observed that the alkaline solution has a significant effect on the tensile strength retention of GFRP stirrups, accounting for 97.8%. The results indicate that GFRP composites are highly vulnerable to alkaline environments, and therefore, a considerable environmental reduction factor must be taken into account when utilising them as reinforcement in concrete structures.

When comparing the impact of temperature with that of solutions, it was observed that raising the temperature can effectively accelerate the degradation mechanism in seawater conditions (accounting for 21.3% contribution). However, in the case of an alkaline solution, the adverse impact of the solution is significantly greater, resulting in a mere 1.8% contribution from the temperature increase. This indicates that GFRP stirrups essentially reach a specific strength retention value after 9 months of conditioning, irrespective of the conditioning temperature. On the other hand, the temperature was found to be a significant factor affecting the tensile strength retention of GFRP stirrups when subjected to the acidic solution (77% contribution). This shows that the aggressive effect of acidic conditions compared to tap water is negligible and the temperature is the main factor responsible for the strength degradation of GFRP stirrups.

5 Conclusion

The study involved testing the effects of different conditions on U-shaped and L-shaped GFRP stirrups with diameters of 6 mm and 8 mm. These stirrups were placed in different solutions, including tap water, seawater, acidic and alkaline solutions, at temperatures of 25, 40, and 60 °C for a period of 9 months. A total of 260 specimens were prepared and tested in tension, and the study examined how the conditioning environments, stirrup shape, and stirrup diameter affected the results. The experimental results were used to draw the following conclusions:

(1) Both the controlled and conditioned samples failed due to weakened strength in the curved part of the stirrup, combined with high-stress concentration during loading, which caused cracks to initiate and propagate towards the straight part, leading to debonding of fibres and resin and ultimately, stirrup failure.
(2) The study found that the alkaline environment had a significant impact on the tensile strength of the stirrups. Regardless of the shape and diameter of the stirrup, exposure to the alkaline environment at temperatures of 25, 40, and 60 °C for 9 months resulted in a reduction of up to 82, 86, and 92%, respectively. This suggests that the alkaline environment is significantly more aggressive compared to other environments studied.
(3) After 9 months at 60 °C, the study found that seawater and acidic solutions were the second and third most aggressive environments, causing the maximum tensile strength reductions of 34 and 22% respectively. In contrast, tap water was identified as the least aggressive environment, resulting in a maximum tensile strength reduction of only 20%.
(4) The study found that L-shaped stirrups generally had higher strength retention values compared to U-shaped stirrups, regardless of their diameter or the environmental conditions to which they were exposed.
(5) The effect of stirrup diameter on their tensile strength durability in harsh environments is negligible.

A notable limitation of the present study is its position as an initial step in the pursuit of aligning accelerated laboratory experiments with real-world conditions to establish safety and environmental reduction factors for design purposes. To address this limitation in future research, the study's next phase could be testing the stirrups at various time intervals. This will involve the application of the Arrhenius theory to develop predictive models for extrapolating data from accelerated aging tests through the incorporation of time-shift factors. The introduction of knock-down factors offers valuable insights into the long-term performance of FRP stirrups in realistic environmental settings.

Another limitation of the current study pertains to the distinction between accelerated aging solution-based tests and the distinct degradation levels and mechanisms witnessed in actual concrete conditions. While the accelerated aging test method employed in this study is well-established and widely accepted, it is acknowledged that this controlled laboratory environment may not precisely mirror the intricate processes observed in real-life concrete settings. This disparity underscores a significant avenue for future research, primarily focused on establishing a direct correlation between the results obtained from accelerated aging tests and the real-world performance of FRP stirrups in concrete environments.

Acknowledgements The support of Dr. Asghar Vatani Oskouei in terms of providing the materials, technical advice and resources is greatly acknowledged.

Funding Open Access funding enabled and organized by CAUL and its Member Institutions. This work was supported by Shahid Rajaee Teacher Training University under grant number 4949.

Declarations

Conflict of interest The authors state that they have no conflict of interest.

Ethical approval This article does not contain any studies with human participants or animals performed by any of the authors.

References

1. Oskouei AV, Bazli M, Ashrafi H, Imani M (2018) Flexural and web crippling properties of GFRP pultruded profiles subjected to wetting and drying cycles in different sea water conditions. Polym Testing 69:417–430
2. Li Y, Teng J, Zhao X, Raman RS (2018) Theoretical model for seawater and sea sand concrete-filled circular FRP tubular stub columns under axial compression. Eng Struct 160:71–84
3. Ozbakkaloglu T, Akin E (2012) Behavior of FRP-confined normal-and high-strength concrete under cyclic axial compression. J Compos Constr 16(4):451–463
4. Doostmohamadi A, Karamloo M, Oskouei AV, Shakiba M, Kheyroddin A (2022) Enhancement of punching strength in GFRP reinforced single footings by means of handmade GFRP shear bands. Eng Struct 262:114349
5. Lam L, Teng J, Cheung C, Xiao Y (2006) FRP-confined concrete under axial cyclic compression. Cement Concr Compos 28(10):949–958
6. Wang Z, Zhao X-L, Xian G, Wu G, Raman RS, Al-Saadi S (2018) Effect of sustained load and seawater and sea sand concrete environment on durability of basalt-and glass-fibre reinforced polymer (B/GFRP) bars. Corros Sci 138:200–218
7. Hosseini SM, Shakiba M, Bazli M, Javaheri A (2022) Using four-point flexure test to investigate effects of temperature and bar size on the tensile properties of GFRP bars. Polym Testing 112:107627
8. Shakiba M, Oskouei AV, Karamloo M, Doostmohamadi A (2021) Effect of mat anchorage on flexural bonding strength between concrete and sand coated GFRP bars. Compos Struct 273:114339
9. Shakiba M, Hosseini SM, Bazli M, Mortazavi SMR, Ghobeishavi MA (2022) Enhancement of the bond behaviour between sand coated GFRP bar and normal concrete using innovative composite anchor heads. Mater Struct 55(9):236
10. Bazli M, Zhao X-L, Bai Y, Raman RS, Al-Saadi S (2019) Bond-slip behaviour between FRP tubes and seawater sea sand concrete. Eng Struct 197:109421
11. Bazli M, Zhao X-L, Jafari A, Ashrafi H, Bai Y, Raman RS, Khezrzadeh H (2020) Mechanical properties of pultruded GFRP profiles under seawater sea sand concrete environment coupled with UV radiation and moisture. Constr Build Mater 258:120369
12. Hoseinzade M, Esfahani M, Arbab F, Shakiba M, Yekrangnia M (2022) Residual flexural capacity of pre-cracked RC beams exposed to chloride penetration at the sea surface temperature. Constr Build Mater 343:128126
13. Imjai T, Garcia R, Guadagnini M, Pilakoutas K (2020) Strength degradation in curved Fiber-reinforced Polymer (FRP) bars used as concrete reinforcement. Polymers 12(8):1653
14. Imjai T (2007) Design and analysis of curved FRP composites as shear reinforcement for concrete structures. The University of Sheffield, England
15. Bazli M, Li Y-L, Zhao X-L, Raman RKS, Bai Y, Al-Saadi S, Haque A (2020) Durability of seawater and sea sand concrete filled filament wound FRP tubes under seawater environments. Compos B Eng 202:108409
16. Shakiba M, Bazli M, Karamloo M, Doostmohamadi A (2023) Bond between sand-coated GFRP bars and normal-strength, self-compacting, and fiber-reinforced concrete under seawater and alkaline solution. J Compos Constr 27(1):04022098
17. Ahmadi H, Shakiba M, Mortazavi SMR, Bazli M, Azimi Z (2023) Feasibility of using static-cast concrete transmission poles fully reinforced with glass-fibre reinforced polymer bars and stirrups: a case study. Case Stud Constr Mater 18:e01780
18. Shakiba M, Ahmadi H, Mortazavi SMR, Bazli M, Azimi Z (2023) A case study on the feasibility of using static-cast fibre-reinforced concrete electric poles fully reinforced with glass fibre reinforced polymer bars and stirrups. Results Eng 17:100746
19. Bazli M, Ashrafi H, Oskouei AV (2016) Effect of harsh environments on mechanical properties of GFRP pultruded profiles. Compos B Eng 99:203–215
20. Wang Z, Zhao X-L, Xian G, Wu G, Raman RKS, Al-Saadi S (2018) Effect of sustained load and seawater and sea sand concrete environment on durability of basalt- and glass-fibre reinforced polymer (B/GFRP) bars. Corros Sci 138:200–218
21. Lu Z, Su L, Xian G, Lu B, Xie J (2020) Durability study of concrete-covered basalt fiber-reinforced polymer (BFRP) bars in marine environment. Compos Struct 234:111650
22. Ceroni F, Cosenza E, Gaetano M, Pecce M (2006) Durability issues of FRP rebars in reinforced concrete members. Cement Concr Compos 28(10):857–868
23. Shakiba M, Bazli M, Karamloo M, Mortazavi SMR (2022) Bond-slip performance of GFRP and steel reinforced beams under wet-dry and freeze-thaw cycles: the effect of concrete type. Constr Build Mater 342:127916
24. Bazli M, Ashrafi H, Oskouei AV (2017) Experiments and probabilistic models of bond strength between GFRP bar and different types of concrete under aggressive environments. Constr Build Mater 148:429–443
25. Ashrafi H, Bazli M, Vatani Oskouei A, Bazli L (2018) Effect of sequential exposure to UV radiation and water vapor condensation and extreme temperatures on the mechanical properties of GFRP bars. J Compos Constr 22(1):04017047
26. Bazli M, Zhao X-L, Bai Y, Raman RS, Al-Saadi S, Haque A (2020) Durability of pultruded GFRP tubes subjected to seawater sea sand concrete and seawater environments. Constr Build Mater 245:118399
27. Bazli M, Jafari A, Ashrafi H, Zhao X-L, Bai Y, Raman RS (2020) Effects of UV radiation, moisture and elevated temperature on mechanical properties of GFRP pultruded profiles. Constr Build Mater 231:117137
28. Bazli M, Zhao X-L, Jafari A, Ashrafi H, Raman RS, Bai Y, Khezrzadeh H (2021) Durability of glass-fibre-reinforced polymer composites under seawater and sea-sand concrete coupled with harsh outdoor environments. Adv Struct Eng 24(6):1090–1109
29. Bazli M, Heitzmann M, Hernandez BV (2022) Durability of Fibre-reinforced polymer-wood composite members: an overview. Compos Struct 295:115827

30. Kazemi H, Yekrangnia M, Shakiba M, Bazli M, Oskouei AV (2022) Bond-slip behaviour between GFRP/steel bars and seawater concrete after exposure to environmental conditions. Eng Struct 268:114796
31. Li S, Guo S, Yao Y, Jin Z, Shi C, Zhu D (2021) The effects of aging in seawater and SWSSC and strain rate on the tensile performance of GFRP/BFRP composites: a critical review. Constr Build Mater 282:122534
32. Al-Salloum YA, El-Gamal S, Almusallam TH, Alsayed SH, Aqel M (2013) Effect of harsh environmental conditions on the tensile properties of GFRP bars. Compos B Eng 45(1):835–844
33. Wu W, He X, Yang W, Dai L, Wang Y, He J (2022) Long-time durability of GFRP bars in the alkaline concrete environment for eight years. Constr Build Mater 314:125573
34. Pan Y, Yan D (2021) Study on the durability of GFRP bars and carbon/glass hybrid fiber reinforced polymer (HFRP) bars aged in alkaline solution. Compos Struct 261:113285
35. Zhou J, Chen X, Chen S (2011) Durability and service life prediction of GFRP bars embedded in concrete under acid environment. Nucl Eng Des 241(10):4095–4102
36. Kim H-Y, Park Y-H, You Y-J, Moon C-K (2008) Short-term durability test for GFRP rods under various environmental conditions. Compos Struct 83(1):37–47
37. Micelli F, Nanni A (2004) Durability of FRP rods for concrete structures. Constr Build Mater 18(7):491–503
38. Benmokrane B, Elgabbas F, Ahmed EA, Cousin P (2015) Characterization and comparative durability study of glass/vinylester, basalt/vinylester, and basalt/epoxy FRP bars. J Compos Constr 19(6):04015008
39. Soles CL, Chang FT, Bolan BA, Hristov HA, Gidley DW, Yee AF (1998) Contributions of the nanovoid structure to the moisture absorption properties of epoxy resins. J Polym Sci, Part B: Polym Phys 36(17):3035–3048
40. Chin JW, Nguyen T, Aouadi K (1997) Effects of environmental exposure on fiber-reinforced plastic (FRP) materials used in construction. J Compos Tech Res 19(4):205–213
41. Aboelseoud MA, Myers JJ (2016) Durability of hybrid composite beam bridges subjected to various environmental conditioning. J Compos Constr 20(6):04016045
42. Miyano Y, Nakada M (2020) Accelerated testing methodology for durability of CFRP. Compos Part B: Eng 191:107977
43. Gonenc O (2003) Durability and service life prediction of concrete reinforcing materials. University of Wisconsin, Madison
44. Bradshaw R, Brinson L (1997) Physical aging in polymers and polymer composites: an analysis and method for time-aging time superposition. Polym Eng Sci 37(1):31–44
45. Ashrafi H, Bazli M, Najafabadi EP, Oskouei AV (2017) The effect of mechanical and thermal properties of FRP bars on their tensile performance under elevated temperatures. Constr Build Mater 157:1001–1010
46. Chen Y, Davalos JF, Ray I, Kim H-Y (2007) Accelerated aging tests for evaluations of durability performance of FRP reinforcing bars for concrete structures. Compos Struct 78(1):101–111
47. Bazli M, Zhao X-L, Raman RS, Bai Y, Al-Saadi S (2020) Bond performance between FRP tubes and seawater sea sand concrete after exposure to seawater condition. Constr Build Mater 265:120342
48. Jafari A, Ashrafi H, Bazli M, Ozbakkaloglu T (2019) Effect of thermal cycles on mechanical response of pultruded glass fiber reinforced polymer profiles of different geometries. Compos Struct 223:110959
49. Shekarchi M, Yekrangnia M, Biniaz A, Raftery GM (2021) Effect of elevated temperatures on the compressive behavior of timber filled steel and pultruded GFRP tubes. Compos Struct 271:114135
50. Dong Z, Wu G, Zhao X-L, Zhu H, Lian J-L (2018) Durability test on the flexural performance of seawater sea-sand concrete beams completely reinforced with FRP bars. Constr Build Mater 192:671–682
51. Dong Z, Wu G, Zhao X-L, Zhu H, Lian J-L (2020) The durability of seawater sea-sand concrete beams reinforced with metal bars or non-metal bars in the ocean environment. Adv Struct Eng 23(2):334–347
52. ASTM, ASTM. 2021. Standard test method for tensile properties of fiber reinforced polymer matrix composite bars. D7205/D7205M-21. West Conshohocken, PA: ASTM., 2021
53. Lu C, Ni M, Chu T, He L (2020) Comparative investigation on tensile performance of FRP bars after exposure to water, seawater, and alkaline solutions. J Mater Civ Eng 32(7):04020170
54. Al Rifai M, El-Hassan H, El-Maaddawy T, Abed F (2020) Durability of basalt FRP reinforcing bars in alkaline solution and moist concrete environments. Constr Build Mater 243:118258
55. Xie J, Li Y, Lu Z, Fan Z, Li J, Li S (2022) Effects of immersion in water, alkaline solution, and seawater on the shear performance of basalt FRP bars in seawater–sea sand concrete. J Compos Constr 26(2):04021071
56. Duo Y, Liu X, Liu Y, Tafsirojjaman T, Sabbrojjaman M (2021) Environmental impact on the durability of FRP reinforcing bars. J Build Eng 43:102909
57. Li Y, Liu X, Li J (2017) Bond properties of FRP-concrete interface with nano-modified epoxy resin under wet-dry cycles. KSCE J Civ Eng 21(4):1379–1385
58. Robert M, Wang P, Cousin P, Benmokrane B (2010) Temperature as an accelerating factor for long-term durability testing of FRPs: should there be any limitations? J Compos Constr 14(4):361–367
59. ACI, ACI-440.3R, Guide test methods for fibre-reinforced polymers (FRPs) for reinforcing or strengthening concrete structures, ACI Committee 440, Farmington Hills, M1 (2012). 2012
60. Ahmed EA, El-Sayed AK, El-Salakawy E, Benmokrane B (2010) Bend strength of FRP stirrups: comparison and evaluation of testing methods. J Compos Constr 14(1):3–10
61. Manalo A, Alajarmeh O, Ferdous W, Benmokrane B, Sorbello C-D, Gerdes A (2022) Effect of simulated hygrothermal environment on the flexural and interlaminar shear strength of particulate-filled epoxy-coated GFRP composites. Constr Build Mater 339:127687
62. Abanilla MA, Karbhari VM, Li Y (2006) Interlaminar and intralaminar durability characterization of wet layup

carbon/epoxy used in external strengthening. Compos B Eng 37(7–8):650–661
63. Fam A, Boles R, Robert M (2016) Durability in a salt solution of pultruded composite materials used in structural sections for bridge deck applications. J Bridg Eng 21(1):04015032
64. Kafodya I, Xian G, Li H (2015) Durability study of pultruded CFRP plates immersed in water and seawater under sustained bending: Water uptake and effects on the mechanical properties. Compos B Eng 70:138–148
65. Bagherpour S, Bagheri R, Saatchi A (2009) Effects of concentrated HCl on the mechanical properties of storage aged fiber glass polyester composite. Mater Des 30(2):271–274